Sensors & Actuators: B. Chemical 280 (2019) 201–209

Contents lists available at ScienceDirect

Sensors and Actuators B: Chemical

journal homepage: www.elsevier.com/locate/snb

Wireless pressure sensor integrated with a 3D printed polymer stent for smart health monitoring

Jongsung Park[a], Ji-Kwan Kim[b], Dong-Su Kim[a], Arunkumar Shanmugasundaram[a], Su A Park[c], Sohi Kang[d], Sung-Ho Kim[d], Myung Ho Jeong[e], Dong-Weon Lee[a,f,*]

[a] MEMS Nanotechnology Laboratory, School of Mechanical Engineering, Chonnam National University, Gwangju, 61186, Republic of Korea
[b] Division of Mechanical & Mold Engineering, Gwangju University, Gwangju, 61743, Republic of Korea
[c] Department of Nature-Inspired Nanoconvergence Systems, Nanoconvergence Mechanical System Division, Korea Institute of Machinery and Materials, Daejeon, 34103, Republic of Korea
[d] Department of Veterinary Anatomy, College of Veterinary Medicine, Chonnam National University, Gwangju, 61186, Republic of Korea
[e] The Heart Research Center of Chonnam National University Hospital, Gwangju, 61469, Republic of Korea
[f] Center for Next-Generation Sensor Research and Development, Chonnam National University, Gwangju, 61186, Republic of Korea

ARTICLE INFO

Keywords:
Wireless pressure sensor
Stent
3D print
Health monitoring
Pressure sensor

ABSTRACT

The primary objective of this study was to deploy a promising wireless pressure sensor system capable of monitoring real-time biological signals in an experimental object. MEMS-based micromachining technology was used to fabricate the proposed SU-8 wireless pressure sensor. The sensor utilizes a capacitor-inductor resonant circuit that can operate the sensor without any external power supply. The variable capacitor in the pressure sensor is designed to change the resonance frequency (130, 183 MHz) in response to applied pressure. The fabricated wireless pressure sensor was integrated into a polymer-based smart stent to minimize the discomfort of medication administration and hospital visits. A 3D bio-printing-based manufacturing technique was employed for the production of a smart polymer stent with complicated shapes. The proposed method is considerably more comfortable than the conventional metal stents fabrication process. The polymer smart stent made of the biocompatible polycaprolactone (PCL) material which can be fully absorbed by the body after a medication period. After integrating the fabricated wireless pressure sensor with the polymer smart stent, various basic experiments such as the working distance of the sensor were performed using a simple experimental setup. The biocompatibility of the proposed polymer stent and the wireless pressure sensor was also successfully confirmed using an experimental animal. The preliminary investigation results indicate that the proposed wireless sensor can be used to obtain necessary information in various parts of the human body as well as the stent.

1. Introduction

The typical atherosclerotic cardiovascular disease is characterized by the formation of plaques and narrowing of the inner walls of the blood vessels causing death by myocardial infarction, transient cerebral ischemic attacks, and stroke [1–3]. According to the World Health Organization, 17.3 million people died of cardiovascular disease in 2008, among whom 7.3 million deaths occurred following myocardial infarction; stroke alone was responsible for 6.2 million deaths. To overcome these issues, a balloon catheter or a stent is used to expand the blood vessel physically. Commercially available metal stents have mesh structures and are manufactured from long metal pipes using a laser-based fabrication technique. The implanted metal stents expand the blood vessel diameter by inflating a balloon. However, mechanical expansion of the metal stent creates a series of side-effects to the patient. Generally, the neointima grows due to thrombus in the peripheral portion of the blood vessel, causing a new narrowing of the inner diameter of the blood vessel [4,5].

Over the years, several research efforts have been devoted to overcoming these complexities [6,7]. Among these studies, the drug-eluting stents (DES) received considerable attention as an effective treatment with the advantage of being able to coat a drug on the stent and deliver the drug directly to the affected area [8,9]. DES is effective in suppressing thrombosis in the early stages. However, the drawback

* Corresponding author at: MEMS Nanotechnology Laboratory, School of Mechanical Engineering, Chonnam National University, Gwangju, 61186, Republic of Korea.
E-mail address: mems@jnu.ac.kr (D.-W. Lee).

https://doi.org/10.1016/j.snb.2018.10.006
Received 1 May 2018; Received in revised form 16 September 2018; Accepted 2 October 2018
Available online 03 October 2018
0925-4005/

of these stents is the availability of limited amounts of drugs, as they are coated on the surface of Co-Cr based metal stent struts [10]. For this reason, patients need to take thrombolytic drugs after a certain period. Also, the inserted metal stents need to be regularly monitored using X-ray-based inspection systems. To address these issues, many researchers are developing biodegradable stents [11,12]. The biodegradable stent is fabricated by using various advanced manufacturing techniques including 3D printing technology [13]. Among the several biodegradable stents, PCL-based biodegradable stents have substantial advantages, including simple manufacturing process for complex shapes, mechanical durability compared to the metal stents, and applicability as drug-eluting stents [13,14].

Developing effective wireless pressure sensor is required in several applications, including biomedical devices, environmental monitoring, and industrial processes. In general, MEMS-based pressure sensors exhibit high reliability, low manufacturing cost and ease of integration with integrated circuits than conventional mechanical sensors. Due to these excellent properties, the medical implant MEMS-based pressure sensors for measuring bio-signals have received substantial attention, and this perspective has been confirmed in a wide range of applications [1,15–17]. Recently, several MEMS-based pressure sensors have been developed to measure intraocular pressure [18–20], brain pressure [21] and pressure inside the blood vessels. Increasing demand for high sensitivity, long-term monitoring, viable and cost-effective fabrication techniques have stimulated further research and development in the field of MEMS-based wireless pressure sensors.

In the present study, we proposed the fabrication of a biocompatible wireless pressure sensor and a biodegradable polymer-smart stent using advanced 3D fabrication techniques. The fabricated wireless pressure sensor was integrated into the polymer stent. The smart stent platform with the wireless pressure sensor can monitor blood vessel pressure in real-time. The unique design of the smart stent allows minimization of periodic medical examinations and controls the dose of drugs after inserting the stent. The preliminary investigations of the fabricated device using an experimental rate demonstrated that the proposed device could be potentially used for health monitoring applications.

2. Sensor mechanism and design

The wireless pressure sensor is fabricated based on the principle of the inductor-capacitor resonant circuit. Fig. 1 shows the schematic diagram of the proposed inductor-capacitor circuit, in which the inductor and capacitor coil is coupled together in a series connection. The inductor coils are designed as planner spirals to reach high impedance value by taking advantage of mutual inductance effect. The magnitude of the generated inductance is strongly dependent on several factors, including the arrangement of the inductor coil, size, separation distance, and shape of the coil. After several trial experiments, the optimized inductance values were obtained and 18- and 30-turn inductor coils were found to be ideal for our applications. The capacitor in the LC circuit consisted of 1 mm round parallel plates. When the external circuit resonates with an internal inductor coil, an electromagnetic force is produced in the inductor coil according to Faraday's law [22]. The generated electromagnetic force induces a current for its self-operation without the use of a battery. As is currently well-established, the maximum electromagnetic force and current will be observed near the resonant frequency of the device. The gap between the two capacitor plates is linearly deformed according to the applied pressure, resulting in a change in capacitance of the capacitor. The change in capacitance reflects in the sensor's resonant frequency, and it is measured by the external circuit. The resonance frequency of the ideal sensor based on LC circuit can be described as Eq. (1) [15], where L_S and C_S is the inductance and capacitance of the device, and ω_0 is the resonance frequency of the device.

$$\omega_0 = 2\pi f_0 = \frac{1}{\sqrt{L_s C_s}} \quad (1)$$

The fabricated wireless pressure sensors were used to monitor the biological signal from an experimental object. The 30-turn inductor coil integrated wireless pressure sensor was designed to measure the biological pressure on the skin or under the skin surface. The length (l), width (w) and the thickness of the sensor were approximately 6.04 mm, 6.10 mm, and 0.15 mm respectively. Another wireless pressure sensor with the 18-turn inductor coil was also designed to measure the pressure inside the blood vessel. The dimensions of the 18-turn inductor coil wireless pressure sensor was approximately 4.66 mm in length, 4.60 mm in width and thickness of 0.15 mm. The finite element method (FEM) analysis of the fabricated wireless pressure sensor was obtained from a previous study [23]. The results were expected to have the same values as the fabricated wireless pressure sensors with the same capacitor dimensions [23]. However, the novelty of the present study was in the sensor fabrication that was undertaken using an improved SU-8 thermal bonding process method. The fabricated wireless pressure sensors showed a uniform capacitor gap distance, as well as high sensing accuracy, compared to values in the previous report.

The inductor coil and capacitor plates of the wireless pressure sensor were made of gold and copper with thicknesses of 100 nm and 10 μm, respectively. The estimated inductance values of the 30-turn and 18-turn wireless pressure sensors were ~3480 nH and ~1230 nH, respectively. The measured capacitance value of the wireless pressure sensor was ~23.18 pF when the capacitor gap distance maintained at 10 μm. The resonant frequencies of the 30-turn and 18-turn sensors were ~142 MHz and ~179 MHz, respectively.

3. Fabrication of the wireless pressure sensor and the polymer stent

The wireless pressure sensor was fabricated on a 4-inch silicon wafer by conventional MEMS techniques. The advanced fabrication techniques enabled the production of a uniform capacitor (see detail in supporting information. Fig. S1-4) and a wireless pressure sensor with high sensing accuracy. The variable capacitor was fabricated employing E-beam deposition on the SU-8 plate, and the inductor coil was formed by a Cu electroplating process. The previously reported wireless pressure sensor fabrication process [23] used a thin layer of inductor coil pattern, and electroplating was later performed to produce a thick coil. The main drawback of the aforementioned paper was the uneven thickness and high resistance of the inductor coil. In the present study, these disadvantages have been carefully taken care off. During the fabrication process of the wireless pressure sensor, an AZ4620 photosensitive polymer was used throughout the Cu layer to make an inductor coil pattern, and then a co-inductor coil pattern was made by an electroplating process.

Fig. 2 illustrates a process flow for fabrication of the wireless pressure sensor. A 4-inch silicon (Si) wafer was used as a substrate. Firstly, a ~300 nm thick SiO2 sacrificial layer was grown on the silicon substrate through a wet oxidation process. A ~200 nm thick copper (Cu) layer was then deposited on the SiO_2 layer for use as a seed layer of an electroplating process to inductor coils (Fig. 2(a)). mold patterns with 30 μm in width and 10 μm in thickness were formed using an AZ4620 photoresist (Fig. 2(b)). The copper coil with a thickness of ~10 μm was subsequently made through the electroplating of Cu (Fig. 2(c)). After removing the AZ4620 photoresist molds (Fig. 2(d)), the SU-8 3010 was covered on the Cu coils and patterned using a photolithography process as shown in Fig. 2(e). This SU-8 layer was employed as a top part of the wireless pressure sensor and the thickness was maintained at 100 μm. Next, the SiO_2 sacrificial layer was removed from the Si wafer using a buffered HF solution, completing the top SU-8 layer of pressure sensors (Fig. 2(f)). For the fabrication of a bottom SU-8 layer, the 10-μm thickness SU-8 layer was coated on the SiO_2 layer of

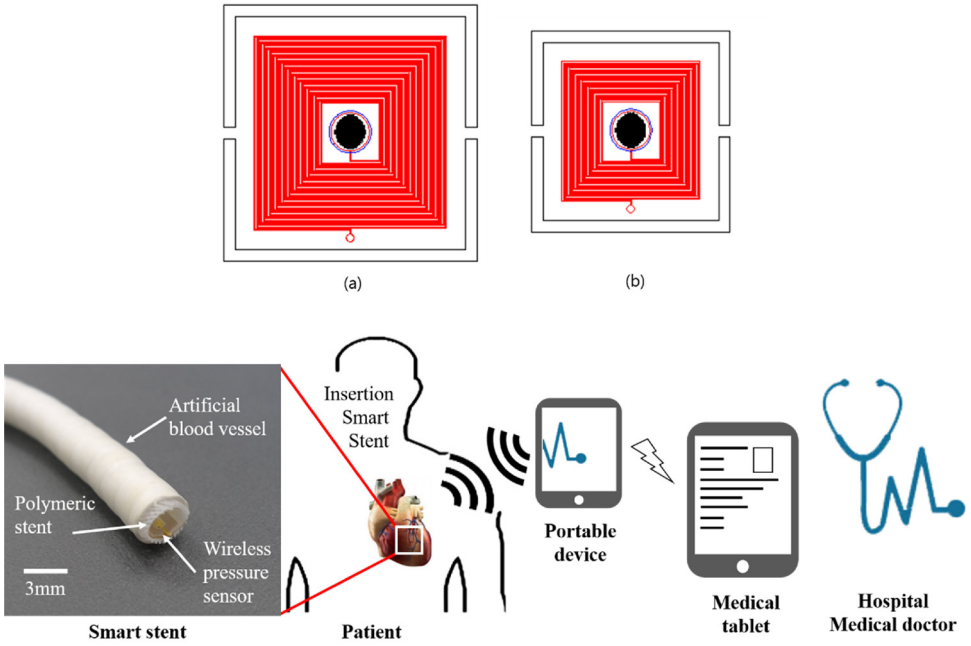

Fig. 1. Schematic representation of the wireless pressure sensor with (**a**) 30-turn and (**b**) 18-turn inductor coils, and **(c)** operating principle of the smart stent.

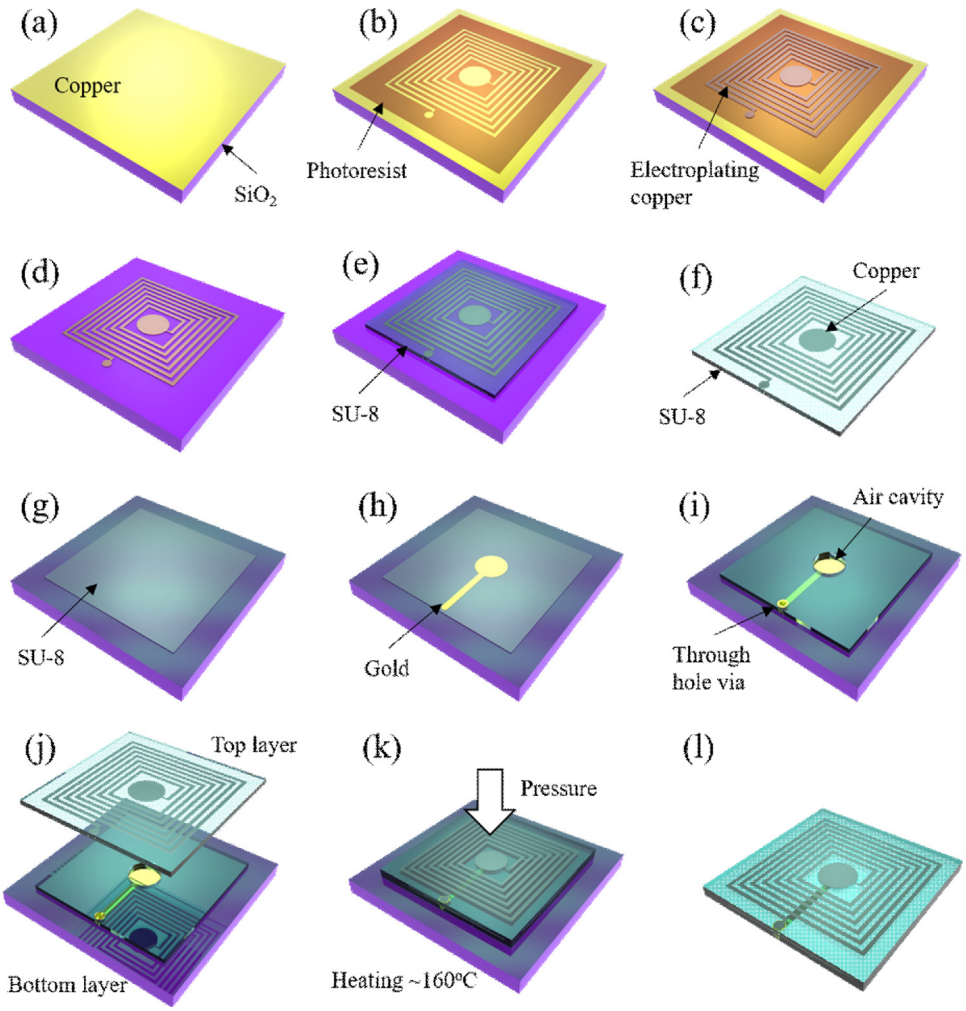

Fig. 2. Process flow of the wireless pressure sensor: (a) deposition of thin Cu layer on a first Si wafer, (b) PR mold for selective electroplating of Cu coil, (c) electroplating for 10 μm-thick inductor fabrication, (d) removal of PR mold and thin Cu layer, (e) patterning of SU-8 photoresist for the use as a top part of pressure sensors, (f) etching of sacrificial SiO2 layer and releasing SU-8 structure from the first Si wafer, (g) patterning of bottom SU-8 layer on a second Si wafer, (h) lift-off process for bottom electrode of capacitor, (i) fabrication of air cavity and through hole via (TSV) using 10 μm-thick SU-8 layer, (j) aligning top SU-8 layer to bottom SU-8 layer, (k) thermal-pressure bonding of top and bottom layers and (l) releasing SU-8 based LC sensor structure from the second Si wafer.

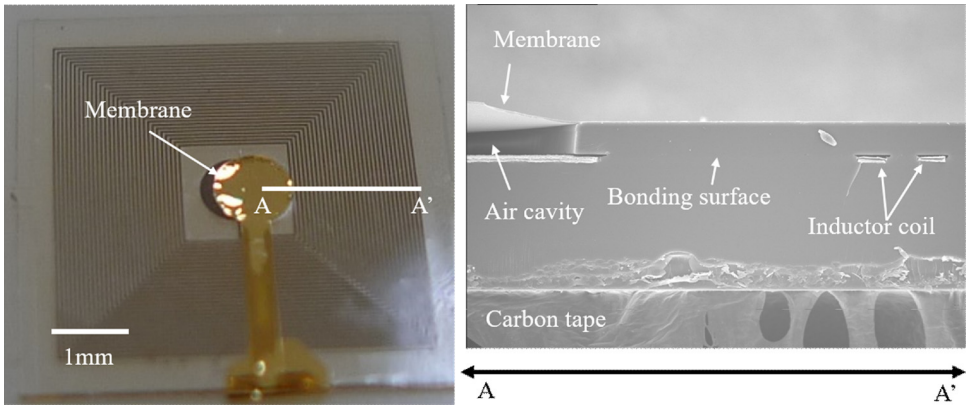

Fig. 3. (**a**) Optical image of the top view of the fabricated wireless pressure sensor, (**b**) SEM cross sectional view of the wireless pressure sensor fabricated using a SU-8 thermal pressure bonding technique.

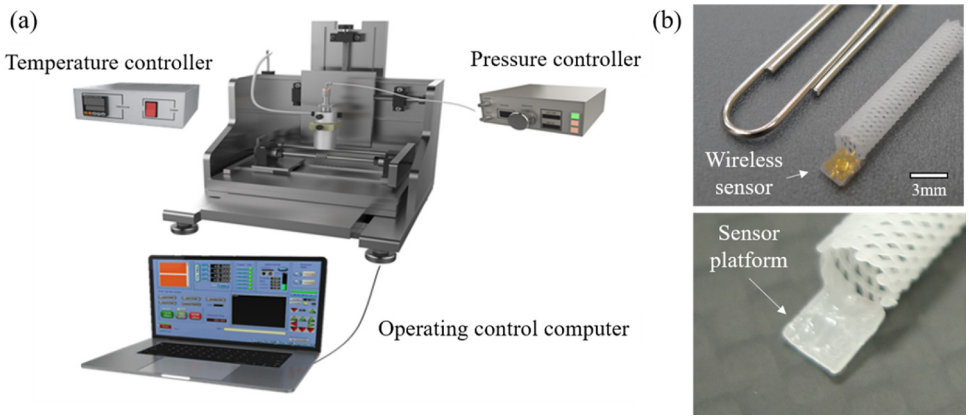

Fig. 4. (**a**) Schematic image illustrating the 3D bio-printing system and (**b**) photograph of the fabricated polymer stent.

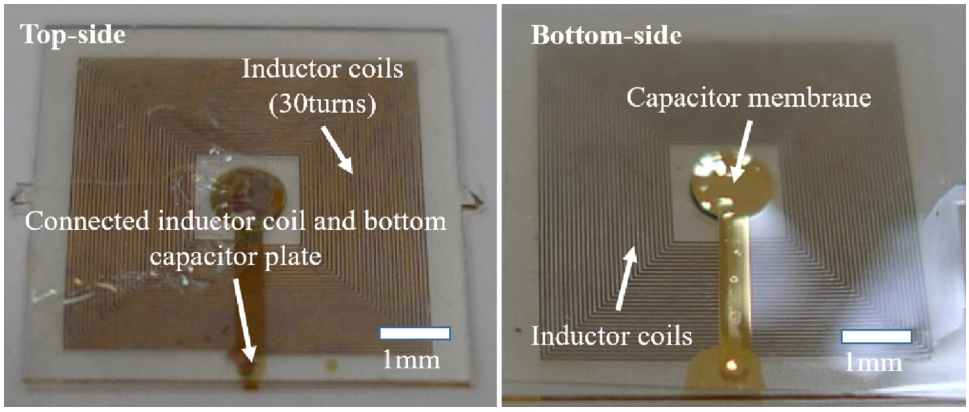

Fig. 5. Optical images illustrating the top and bottom view of the 30-turn wireless pressure sensor.

Table 1
Measurement results of wireless pressure sensors with 18-turn and 30-turn inductor coils.

Parameters	Sensor with 18-turn inductor coil	Sensor with 30-turn inductor coil
Capacitor size	Dia. 1 mm	Dia. 1 mm
Resonance frequency	183 MHz	130 MHz
Phase @ 3 mm	70°	32°
Size (w × h)	4 mm × 4 mm	6 mm × 6 mm
Sensitivity	160 kHz/mmHg	160 kHz/mmHg

another wafer (Fig. 2(g)). Subsequently, Ti/Au layers with 10 nm/100 nm in thickness were deposited using an electron beam evaporator. A bottom electrode for the variable capacitor fabrication was then patterned by a metal etching process (Fig. 2(h)). And then, the same SU-8 photoresist was spin-coated and patterned on the first SU-8 3010 layer to form air cavity of the capacitor structure. As shown in Fig. 2(i), gold (Au) was used to electrically interconnect the top electrode of the capacitor to the Cu coil connected to the bottom electrode of the capacitor. The fabricated top SU-8 layer was aligned to the bottom SU-8 layer formed on the second Si wafer. The pressure sensor structures were then heated for 1 h by applying 850 gf at 160 °C (Fig. 2(j), (k)) [24]. Finally, the sensor structures were released from the second Si wafer by etching the SiO_2 sacrificial layer. The yield and reliability of

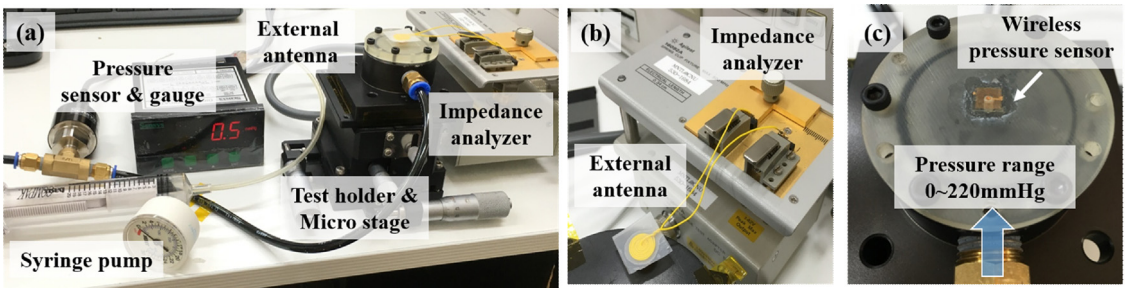

Fig. 6. (a–c) Optical images of the measurement setup used to evaluate wireless pressure sensors.

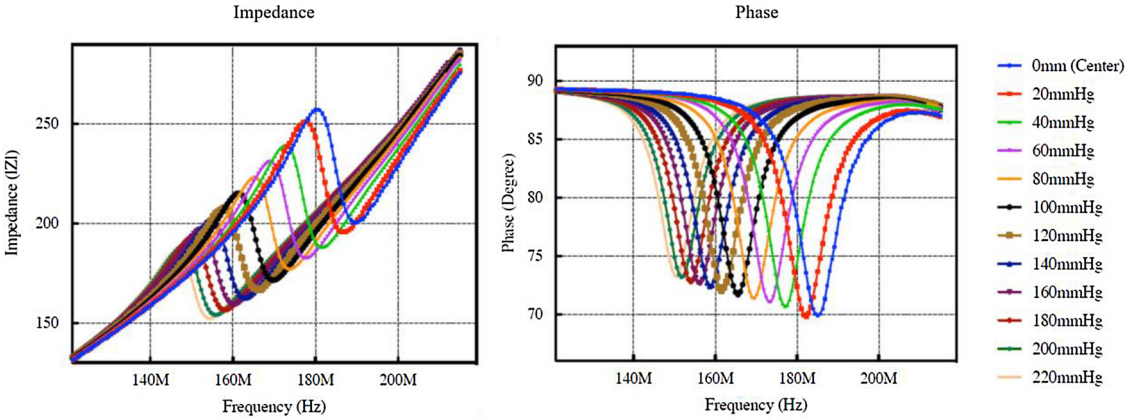

Fig. 7. (a) Impedance and (b) phase changes of the wireless pressure sensor with 18-turn inductor coil as a function frequency at different applied pressure.

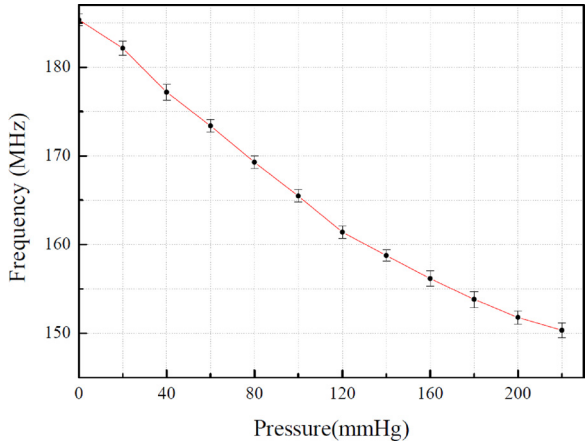

Fig. 8. Resonance frequency change as a function of the applied pressure.

fabricated wireless pressure sensors were greatly improved by employing the thermal bonding in a compressed state. Fig. 3 shows optical and SEM images of the fabricated wireless pressure sensor. The SEM cross-sectional view confirmed the uniform formation of the capacitor and the inductor.

The polymer-based smart stent was made by adopting 3D printing techniques as a manufacturing method. Fig. 4 shows the schematic illustration of the 3D printer setup, consisting of a heating module for heating the plastic materials and a pressure module for the discharging process. Thermal extrusion with the 3D bio-printer provided a tube-type structure to the fabrication of the stent route. The bio-printer was equipped with a dispenser and 4-axes stages were assembled with a temperature and a pressure controller. The controlled temperature and pressure facilitated the formation of the smooth stent architecture. The tube-type stent was fabricated using a biocompatible and biodegradable polycaprolactone (PCL) polymer material [13]. The photograph in Fig. 4(b) shows the fabricated polymer stent with a diameter of ~3 mm and a length of ~13 mm. The small sensor platform was provided with the polymer stent for the integration of the wireless pressure sensor to measure the pressure inside the smart stent.

4. Results and discussion

Fig. 5 illustrates the top and bottom view of the fabricated SU-8-based wireless pressure sensor. Table 1 summarizes the obtained results, i.e., the resonant frequency and sensitivity analysis of both 18-turn and 30-turn wireless pressure sensors. The sensor resonant frequency of the fabricated pressure sensor with the same dimensions has a slight variation in the resonant frequency in the range of 2 ~ 5 MHz. It could be attributed to the difference in current strength depending on the position of the silicon wafer during the electroplating process of the inductor coil. The slight different thickness of a silicon wafer during the sensor fabrication resulted in a difference in the resonant frequency.

The fabricated wireless pressure sensors were characterized by using a custom-designed plastic jig and an impedance analyzer. The series of photographs for the preliminary experiment are shown in Fig. 6. As shown in Fig. 6(c), the fabricated pressure sensor was glued to the jig connected to a syringe pump. The external pressure in the range of 0 ~ 200 mmHg at a pressure interval of 20 mmHg was then applied to the pressure sensor. Resonant frequency of the pressure sensor with respect to the applied pressure was transmitted to the impedance analyzer (Agilent 4395 A) through the external antenna. A micro-stage was employed to assess the positional alignment of the wireless pressure sensor to the external antenna.

Resonance frequencies of two different wireless pressure sensor with 18-turn and 30-turn inductors were investigated. Fig. 7 shows the change of resonance frequency for the wireless pressure sensor with 18 turns inductor as a function of applied pressures in the range of 0 to 220 mmHg. The maximum error range of the pressure sensor was ~2% as shown in Fig. 8. As observed in Fig. 8, when the applied pressure is higher than 180 mmHg, the resonance frequency of the pressure sensor

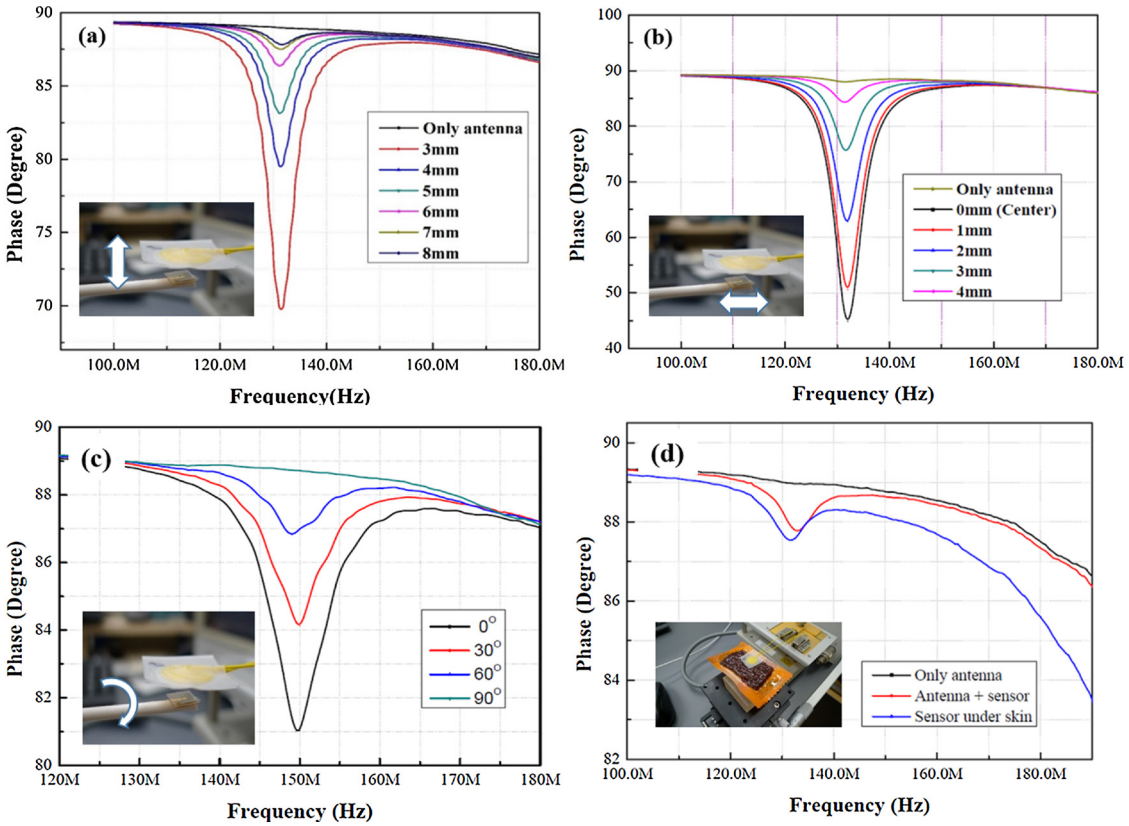

Fig. 9. Sensitivity of the wireless pressure sensor with the 30-turn inductor coil as a function of various applied frequencies under various measurement conditions (**a**) vertical, (**b**) horizontal, (**c**) tilt and (**d**) phantom tissue.

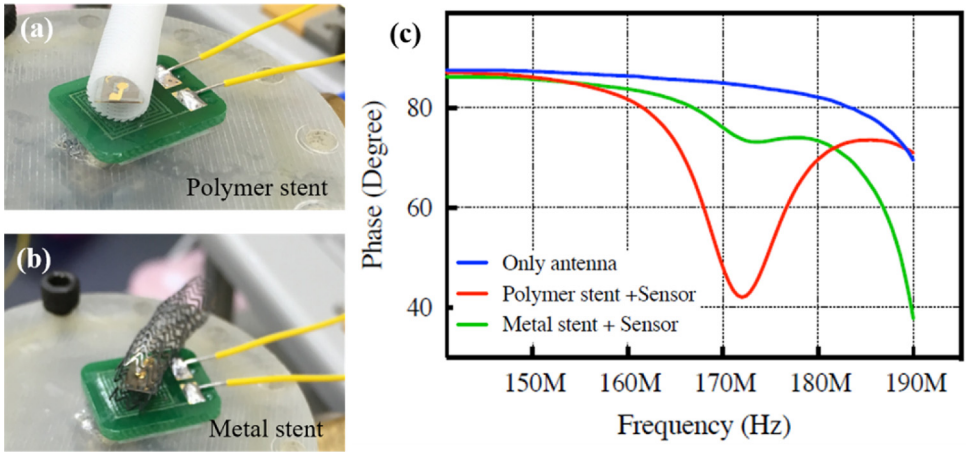

Fig. 10. (**a**, **b**) Photographs illustrating the developed wireless pressure sensor integrated 3D printed polymer and metal stents, (**c**) sensitivity analysis of the wireless pressure sensor integrated smart stent and metal stent.

begins to deviate from the linear change. This is because the value of the variable capacitor changes non-linearly at high pressure or large deformation. However, the non-linear change of the resonance frequency can be ignored in the general range of use of the fabricated wireless pressure sensor because it deviates from a normal blood pressure range. The measured resonance frequencies of the pressure sensors with the 18-turn and 30-turn inductor coils were 183 MHz and 130 MHz, respectively. The sensitivity of both wireless pressure sensors found were ~160 kHz/mmHg. Owing to the same capacitor plate dimensions and air cavity, both the sensors possessed the same sensitivity range.

The sensitivity of the 30-turn inductor coil integrated wireless pressure sensor was investigated according to the distance between the wireless pressure sensor and the external antenna. To assess the sensitivity, the sensor position was fixed and we adjusted the position of the external antenna. The sensitivity range of the pressure sensor was evaluated by measuring the phase changes at various measurement conditions.

The sensitivity of the pressure sensor varied according to its alignment with the external antenna. Therefore, the sensitivity of the pressure sensor according to its different positions: *(i)* vertical, *(ii)* horizontal, and *(iii)* slope (Fig. 9) were evaluated. Firstly, the wireless pressure was aligned vertically to the external antenna. The difference in phase angle of the pressure sensor was evaluated in an air medium by increasing the distance between the sensor and the antenna using a micro-stage. The sensitivity of the sensor was found to be 3° when the

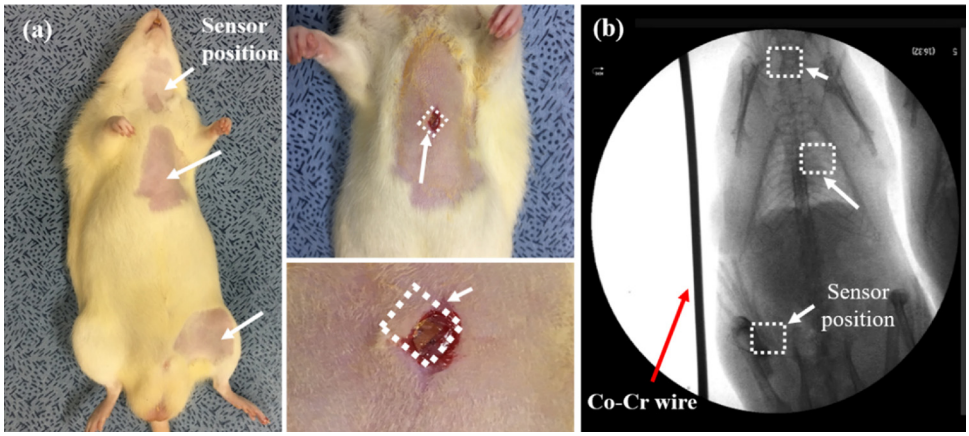

Fig. 11. Photograph of the wireless pressure sensor inserted into the experimental animal. (**a**) The arrow mark indicates the surgical location of the inserted wireless pressure sensors and (b) biocompatibility test of the experimental rate carried out using X-ray-based imaging analysis.

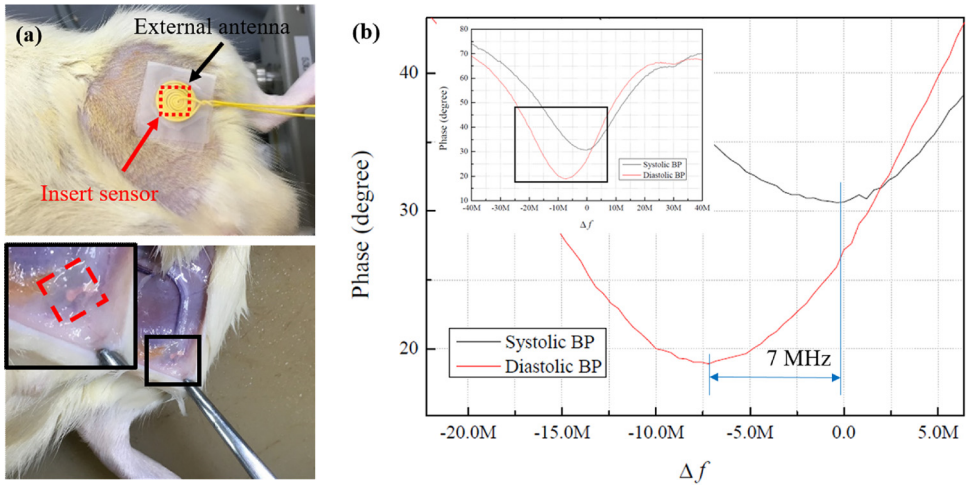

Fig. 12. Evaluation of biocompatibility of the wireless pressure sensor using an experimental animal. (**a**) biocompatibility check and (**b**) blood pressure measurement of the experimental animal monitored using an implanted wireless pressure sensor.

distance between the sensor and the external antenna was ~8 mm (Fig. 9(a)). The sensitivity of the wireless pressure sensor in a horizontal position was ~5° at 3 mm (Fig. 9(b)). In tilt positions, the sensitivity of the sensor was ~2° when the angle between the pressure sensor and antenna was 60° (Fig. 9(c)). The medium between the wireless pressure sensor and the external antenna was also an important factor that determined the sensitivity of the pressure sensor. Therefore, the pressure sensor was placed in a phantom tissue, and the sensitivity of the sensor was evaluated. The obtained results using a phantom tissue are shown in Fig. 9(d). These investigations directly implied that the magnitude of the sensor sensitivity was greatly influenced by its differential placement and environmental conditions with respect to the external antenna. Although the pressure sensor positions and environmental circumstances varied, the obtained results from the sensor were confirmed to be in the acceptable range.

The main objective of this research work was to develop a wireless pressure sensor integrated smart stent to monitor biological signals from an experimental object. Generally, metallic stents are widely employed to expand the blood vessels. However, when integrating wireless pressure sensors into conventional metallic stents, it is difficult to measure the resonant frequency signals because they are reflected or scattered by the metal stents. To overcome these drawbacks, biodegradable polymer materials were used as the material of the stent. Fig. 10(a) and (b) show photographs of the fabricated wireless pressure sensors integrated with polymeric and metallic stents. The sensitivity of the various smart stents was investigated using a simple experimental setup. In the evaluation of the smart stents, the 18-turn coil of the wireless pressure sensor was employed during the experiments due to the smaller inner diameter of conventional stents. As shown in Fig. 10(c), the sensitivity of the polymer stent integrated with the wireless pressure sensor was better than that of the wireless pressure sensor integrated metal stent. The obtained experimental results revealed the feasibility of using the fabricated wireless pressure sensor integrated polymer stent for real-time monitoring applications.

Finally, the *in vivo* biocompatibility of the fabricated wireless pressure sensor was investigated to demonstrate the feasibility of using the sensor inside blood vessels. All animal tests were carried out in accordance with the procedures approved by the animal care committee at the Chonnam National University-South Korea and confirmed with the guidelines of the US National Institutes of Health. The fabricated wireless pressure sensors were inserted into various locations, including the neck, heart, and femoral areas of the experimental animal (Fig. 11(a)). The biocompatibility of the pressure sensors was investigated for more than 3 months. During the evaluation period, the experimental mouse was monitored at regular intervals through X-ray-based imaging analysis. The X-ray observations (Fig. 11(b)) showed no abnormalities such as tumors or any other biological illness in the experimental animal. The photograph in Fig. 12(a) illustrates the biocompatibility test of the wireless pressure sensor inserted into the experimental animal. The pressure inside the blood vessels of the

experimental animal was monitored using an inserted wireless pressure sensor (Fig. 12(b)). The normal blood pressure range in the animal is approximately 91 ~ 129 mmHg, and the difference between the maximum and minimum blood pressure is approximately 38 mmHg [25]. As shown in Fig. 12(b), the difference between the maximum and the minimum resonant frequency was approximately 7 MHz. The pressure difference calculated from the sensor sensitivity (0.16 MHz/mmHg) was found to be approximately 43 mmHg, a value similar to that of the normal blood pressure for the experimental animal.

Reproducibility and robustness of the wireless pressure sensors are very important for practical use of the sensors. To ensure the long-term reliability, the fabricated wireless pressure sensors were inserted into the experimental animal and the change in blood pressure were measured continuously for more than 3 months. The resonance frequency changes due to the contraction and relaxation of the ventricles over a period of three months are shown in Fig. S5. The obtained experimental results clearly indicate the repeatable measurement of the pressure change by using the resonance frequency shift in a range of ~3-7 MHz. In order to measure the pressure value precisely, the experimental animal was anesthetized and the measurement was carried out, which showed a slight deviation from the steady state pressure of the experimental rat. The preliminary study suggested the possibility of using the fabricated wireless pressure sensor and polymer stent in a human body. Even though the consequences do not accurately simulate those of a human, the obtained results are crucial for the assessment of safety and deliver valuable information regarding pathological studies.

5. Conclusions

We successfully fabricated a wireless pressure sensor and polymer-based smart stent for biomedical applications. The SU-8 wireless pressure sensor was developed through the MEMS-based fabrication technique to achieve miniaturization and stable production of the device. The biocompatible polycaprolactone-based smart stent was developed using 3D printing technology. The proposed stent fabrication process is easy to create complex shapes and structures. The fabricated wireless pressure sensor was integrated into the polymer smart stent and was verified through biocompatibility tests. The produced wireless pressure sensor was investigated in detail through various analyses and *in-vivo* biocompatibility tests in an experimental animal. Furthermore, we also conclusively demonstrated the possibility of measuring the intravascular blood pressure of the experimental animal. We anticipate that the proposed wireless pressure sensor and smart stent will present opportunities to develop the next generation of biomedical devices for health monitoring applications.

Acknowledgments

This study was supported by a grant from the Korean Health Technology R&D Project, Ministry of Health and Welfare (HI13C1527) and the National Research Foundation of Korea grant (2017R1E1A1A01074550) funded by the Korea government.

Appendix A. Supplementary data

Supplementary material related to this article can be found, in the online version, at doi:https://doi.org/10.1016/j.snb.2018.10.006.

References

[1] X. Chen, B. Assadsangabi, Y. Hsiang, K. Takahata, Enabling angioplasty-ready "Smart" stents to detect in-stent restenosis and occlusion, Adv. Sci. 5 (2018) 170056.
[2] World Health Organization, Prevention of Cardiovascular Disease, World Health Organization, 2007.
[3] A.D. Lopez, C.D. Mathers, M. Ezzati, D.T. Jamison, C.J. Murray, Global and regional burden of disease and risk factors, 2001: systematic analysis of population health data, Lancet 367 (2006) 1747–1757.
[4] N. Glenn Levine, P. Andrew, L. Joseph, Restenosis following coronary angioplasty: clinical presentations and therapeutic options, Clin. Cardiol. 18 (1995) 693–703.
[5] U. Rauch, J.I. Osende, V. Fuster, J.J. Badimon, Z. Fayad, J.H. Chesebro, Thrombus formation on atherosclerotic plaques: pathogenesis and clinical consequences, Ann. Intern. Med. 134 (2011) 224–238.
[6] S.I. Negi, R. Torguson, J. Gai, S. Kiramijyan, E. Koifman, R. Chan, P. Randolpg, A. Pichard, L.F. Satler, R. Waksman, Intracoronary brachytherapy for recurrent drug-eluting stent failure, JACC-Cardiovasc. Interv. 9 (2016) 1259–1265.
[7] T.F. Lüscher, J. Steffel, F.R. Eberli, M. Joner, G. Nakazawa, F.C. Tanner, R. Virmani, Drug-eluting stent and coronary thrombosis: biological mechanisms and clinical implications, Circulation 115 (2007) 1051–1058.
[8] P. Vermeersch, P. Agostoni, S. Verheye, P. Van den Heuvel, C. Convens, F. Van den Branden, G. Van Langenhove, Increased late mortality after sirolimus-eluting stents versus bare-metal stents in diseased saphenous vein grafts: results from the randomized DELAYED RRISC Trial, J. Am. Coll. Cardiol. 50 (2007) 261–267.
[9] S. Bangalore, B. Toklu, N. Amoroso, M. Fusaro, S. Kumar, E.L. Hannan, F.P. David, F. Feit, Bare metal stents, durable polymer drug eluting stents, and biodegradable polymer drug eluting stents for coronary artery disease: mixed treatment comparison meta-analysis, BMJ 347 (2013) f6625.
[10] R. Kornowski, M.K. Hong, F.O. Tio, O. Bramwell, H. Wu, M.B. Leon, In-stent restenosis: contributions of inflammatory responses and arterial injury to neointimal hyperplasia, J. Am. Coll. Cardiol. 31 (1998) 224–230.
[11] H. Tamai, K. Igaki, E. Kyo, K. Kosuga, A. Kawashima, S. Matsui, K. Hidenori, T. Takafumi, M. Seiichiro, H. Uehata, Initial and 6-month results of biodegradable poly-l-lactic acid coronary stents in humans, Circulation 102 (2000) 399–404.
[12] H. Hermawan, D. Dube, D. Mantovani, Developments in metallic biodegradable stents, Acta Biomater. 6 (2010) 1693–1697.
[13] S.A. Park, S.J. Lee, K.S. Lim, I.H. Bae, J.H. Lee, W.D. Kim, M.H. Jeong, J.K. Park, In vivo evaluation and characterization of a bio-absorbable drug-coated stent fabricated using a 3D-printing system, Mater. Lett. 141 (2015) 355–358.
[14] J. Holländer, N. Genina, H. Jukarainen, M. Khajeheian, A. Rosling, E. Mäkilä, N. Sandler, Three-dimensional printed PCL-based implantable prototypes of medical devices for controlled drug delivery, J. Pharm. Sci. 105 (2016) 2665–2676.
[15] N. Xue, S.P. Chang, J.B. Lee, A SU-8-based microfabricated implantable inductively coupled passive RF wireless intraocular pressure sensor, J. Microelectromech. Syst. 21 (2012) 1338–1346.
[16] X. Sun, Y. Zheng, X. Peng, X. Li, H. Zhang, Parylene-based 3D high performance folded multilayer inductors for wireless power transmission in implanted applications, Sens. Actuator A-Phys. 208 (2014) 141–151.
[17] G. Schwartz, C.K.T. Benjamin, J. Mei, L.A. Anthony, D.H. Kim, H. Wang, Z. Bao, Flexible polymer transistors with high pressure sensitivity for application in electronic skin and health monitoring, Nat. Commun. 4 (2015) 1859.
[18] B. Kang, H. Hwang, S.H. Lee, J.Y. Kang, J.H. Park, C. Seo, C. Park, A wireless intraocular pressure sensor with variable inductance using a ferrite material, J. Semicond. Technol. Sci. 13 (2013) 355–360.
[19] R. Puers, G. Vandevoorde, D.D. Bruyker, Electrodeposited copper inductors for intraocular pressure telemetry, J. Micromech. Microeng. 10 (2000) 124–129.
[20] U. Schnakenberg, P. Walter, G. vom B¨ogel, C. Kr¨uger, H.C. L¨udtke-Handjery, H.A. Richter, W. Specht, P. Ruokonen, W. Mokwa, Initial investigation on systems for measuring intraocular pressure, Sens. Actuator A-Phys. 85 (2000) 287–291.
[21] L.Y. Chen, B.C.K. Tee, A.L. Chortos, G. Schwartz, V. Tse, D.J. Lipomi, H.S.P. Wong, M.V. McConnel, Z. Bao, Continuous wireless pressure monitoring and mapping with ultra-small passive sensors for health monitoring and critical care, Nat. Commun. 5 (2014) 5028.
[22] I. Galili, D. Kaplan, Y. Lehavi, Teaching Faraday's law of electromagnetic induction in an introductory physics course, Am. J. Phys. 74 (2006) 337–343.
[23] J. Park, J.K. Kim, S.J. Patil, J.K. Park, S. Park, D.W. Lee, A wireless pressure sensor integrated with a biodegradable polymer stent for biomedical applications, Sensors 16 (2016) 809.
[24] S. Li, C.B. Freidhoff, R.M. Young, R. Ghodssi, Fabrication of micronozzles using low-temperature wafer-level bonding with SU-8, J. Micromech. Microeng. 13 (2003) 732–738.
[25] E.M. Dantas, E.B. Pimentel, R.V. Andreão, B.S. Cichoni, C.P. Gonçalves, D.D.A. Zaniqueli, D.S. Cichoni, C.P. Goncalves, D.D.A. Zaniqueli, M.P. Baldo, S.L. Rodrigues, J.G. Mill, Carvedilol recovers normal blood pressure variability in rats with myocardial infarction, Auton. Neurosci-Basic Clin. 177 (2013) 231–236.

Dr. Jongsung Park received his Ph.D. degrees in Mechanical engineering from Chonnam National University, Korea in 2018. Now he is a postdoc at MEMS and Nanotechnology Laboratory, Chonnam National University, Korea. His research interests wireless pressure sensor and BioMEMS device.

Prof. Ji-Kwan Kim received his Ph.D. degrees in Mechanical engineering from Chonnam National University, Gwangju, Republic of Korea in 2014. He has been an assistant professor of Mechanical and Metallic Mold Engineering at Gwangju University (GU), Republic of Korea since 2014. At GU, his research interests include smart cantilever devices & Graphene PDMS composite materials.

Dong-Su Kim received his BS degree in electronics engineering from Chosun University, Korea in 2013 and MS in mechanical engineering from Chonnam National University, Korea in 2016. Currently he is pursuing his doctoral degree in mechanical engineering at MEMS and Nanotechnology Laboratory, Department of Mechanical Engineering, Chonnam National University, Korea. His research activity is primarily focused on design and fabrication new class of Bio-MEMS device for drug screening applications.

Dr. Arunkumar Shanmugasundaram has followed up on his dual Master's Degree in 'Physics' and 'Sensor System Technology' with a Ph.D. from CSIR-Indian Institute of Chemical Technology, Hyderabad, India. Currently, he is working as a post-doctoral researcher at MEMS and Nanotechnology Laboratory, School of Mechanical Engineering, Chonnam National University, Korea. His research interests include design and development of functional nanostructured materials for applications in sensors, catalysis, and energy storage device

Dr. Su A Park received her Ph.D. degrees in biomedical engineering from Inje University, Gimhae, Republic of Koera in 2006. She has been a Researcher in Korea Institute of Machinery & Materials (KIMM) since 2006. In 2011, she was a visiting scholar at Department of biomedical engineering of University of California, Davis (UC Davis) in the USA. At KIMM, she researches tissue engineering and regenerative medicine using 3D bioprinting for the artificial organ fabrication.

Dr. Sohi Kang, D.V.M., received her Ph.D. degrees in College of Veterinary Medicine from Chonnam National University (CNU), Gwangju, Republic of Korea in 2018. She has been a Research Professor of Biomaterials Development Center at CNU since 2018. Her research interests include how cancer therapy can impact neuronal morphological and molecular biological changes.

Prof. Sung-Ho Kim, D.V.M., received his Ph.D. degrees in College of Veterinary Medicine from Kyungpook National University, Daegu, Republic of Korea in 1991. He has been a Professor of Veterinary Anatomy at Chonnam National University (CNU), Republic of Korea since 1995. Previously, he was with the Korea Institute of Radiological & Medical Sciences, working mainly on modification of gamma-radiation response. At CNU, his research interests include osteoporosis prevention and treatment, environmental radiation, and radiation protectants.

Prof. Myung Ho Jeong received his M.D. (1983) and Ph.D. (1989) degrees from Chonnam National University, Gwangju, Korea. He has been a professor of Department of Cardiovascular Medicine at Chonnam National University (CNU) since 1992. He was trained as a post-doc fellowship at Mayo Clinic and Mayo Graduate School, USA. His main research fields include interventional cardiology, development of new coronary stents, acute myocardial infarction, atherosclerosis and thrombosis. He is current presidents of Korean Society of Myocardial Infarction, Korean Society of Lipid and Atherosclerosis, Korean Society of Thrombosis and Hemostasis. He is fellows of American College of Cardiology (FACC), American Heart Association (FAHA), European Society of Cardiology (FESC) and Society of Cardiac Angiography and Intervention (FSCAI). He is members of Korea Academy of Science and Technology (KAST) and National Academy of Medicine of Korea (NAMK). He is a director of Heart Research Center nominated by Korea Ministry of Health and Welfare.

Prof. Dong-Weon Lee received his Ph.D. degrees in Mechatronics engineering from Tohoku University, Sendai, Japan in 2001. He has been a Professor of Mechanical Engineering at Chonnam National University (CNU), Republic of Korea since 2004. Previously, he was with the IBM Zurich Research Laboratory in Switzerland, working mainly on microcantilever devices for chemical AFM applications. At CNU, his research interests include smart cantilever devices, miniaturized energy harvesters & flexible supercapacitors, smart structures & materials, and nanoscale transducers. He is a member of the technical program committee of IEEE MEMS conference, IEEE Sensors Conference, Transducers, and Microprocesses and Nanotechnology Conference etc.